Electrically active induced energy levels and metastability of B and N vacancy-complexes in $4H$-SiC

E. Igumbor[1,2*], O. Olaniyan[1], R. E. Mapasha[1], H. T. Danga[1], E. Omotoso[1] and W. E. Meyer[1]

[1]Department of Physics, University of Pretoria, Pretoria 0002, South Africa

[2]Department of Mathematical and Physical Sciences, Samuel Adegboyega University, Ogwa Edo State Nigeria

E-mail: elgumuk@gmail.com

January 2018

Abstract. Electrically active induced energy levels in semiconductor devices could be beneficial to the discovery of an enhanced p or n-type semiconductor. Nitrogen (N) implanted into $4H$-SiC is a high energy process that produced high defect concentrations which could be removed during dopant activation annealing. On the other hand, boron (B) substituted for silicon in SiC causes a reduction in the number of defects. This scenario leads to a decrease in the dielectric properties and induced deep donor and shallow acceptor levels. Complexes formed by the N, such as the nitrogen-vacancy centre, have been reported to play a significant role in the application of quantum bits. In this paper, results of charge states thermodynamic transition level

of the N and B vacancy-complexes in 4*H*-SiC are presented. We explore complexes where substitutional N_{Si}/N_C or B_{Si}/B_C sits near a Si (V_{Si}) or C (V_C) vacancy to form vacancy-complexes (N_CV_C, N_CV_{Si}, $N_{Si}V_C$, $N_{Si}V_{Si}$, B_CV_C, B_CV_{Si}, $B_{Si}V_C$ and $B_{Si}V_{Si}$). The energies of formation of the N related vacancy-complexes shown the N_CV_C to be energetically stable close to the valence band maximum in its double positive charge state. The N_CV_{Si} is more energetically stable in the double negative charge state close to the conduction band minimum. The $N_{Si}V_C$ on the other hand, induced double donor level and the N_CV_{Si} induced a double acceptor level. For B related complexes, the B_CV_C and $B_{Si}V_C$ were energetically stable in their single positive charge state closed to the valence band maximum. As the Fermi energy is varied across the band gap, the neutral and single negative charge states of the $B_{Si}V_C$ become more stable at different energy levels. B and N related complexes exhibited charge state controlled metastability behaviour.

Keywords: Defect, formation energy, charge state, complexes

Submitted to: *J. Phys.: Condens. Matter*

1. Introduction

SiC has different polytypes of which the 2*C*, 3*C*, 4*H* and 6*H* are the most common. The different polytypes of SiC only differ in the stacking order which affects their electronic and optical properties. Earlier reports have shown that all polytypes are inert, hard and have high thermal conductivity [1, 2]. Furthermore, the breakdown

electric field strength, saturated drift velocity or impurity ionization energies are all specific for different polytypes. In this report, 4*H*-SiC is the focus due to its large single crystal that is readily available and its relatively large band gap, which makes it more likely that defect induced electrical levels will occur within the band gap. The 4*H*-SiC is a promising material for high-voltage devices due to its higher bulk mobility and smaller anisotropy compared to other polytypes. The 4*H*-SiC has been experimentally reported to have a wide band gap of 3.26 eV at 300 K. In addition, the 4*H*-SiC is capable of operating at high temperature and high frequency which makes it a suitable substrate material for producing high frequency electronic devices for applications in radiation harsh environments (space, accelerator facilities and nuclear power plants) [1, 2]. Point and extended defects play vital roles in 4*H*-SiC as they have the tendency to either influence or limit its performance. The study of radiation-induced defects in semiconductors is a significant area of research in material science from the point of view of device applications [3]. Defects in 4*H*-SiC semiconductor and its electrically active levels along with the stability within the band gap have been studied experimentally [1, 4, 5] or theoretically [6, 7, 8]. Some of these defects are thermodynamically stable whereas some are unstable. SiC has been reported to have dielectric loss in microwave. This loss can be greatly improved by *p*- or *n*-type doping [5]. For example, Al doping as well as N doping have the tendency to improved the microwave dielectric properties of SiC [9]. Earlier reports suggest that a B atom substituted for Si in SiC causes a reduction in the number of defects, which results in a decrease of the

dielectric properties [10, 11]. Photoluminescence experimental investigation reveals that the Al and B-doped SiC exhibit emission profile below 2.00 eV, implying the existence of acceptor levels. Results of co-doping of N and B in 3*C*-SiC reveal that the deep B acceptor recombines with a shallow nitrogen donor. This shows that the ionised donor and acceptor can occupy the same sub-lattice. In hexagonal 4*H*-SiC, Al and B are passivated by forming complexes with H [12]. Furthermore, B and Al are suggested to be the most important *p*-type dopants in SiC. The Al is more stable in Si site with the tendency of inducing shallow acceptor level between 0.19-0.25 eV above the valence band maximum (VBM). The B on the other hand, induces deep as well as shallow level in SiC occupies Si or C site with a single shallow acceptor and deep donor levels of 0.30 and 0.55 eV above the VBM, respectively [13]. The deep level induced by B has been observed in a photoluminiscene experimental measurement [14]. Various vacancy-complexes have been reported for different semiconductor materials, most especially Ge where donors diffuse via interactions with vacancies [15, 16, 17]. In 3*C*-SiC, vacancy-complexes and other forms of defect clusters have been reported. Notable is the $B_{Si}C_{Si}$, which induces electrically active level with energy of E_V+0.47 eV (E_V is the energy of the VBM) [18]. Reports have shown that for *n*-type doping of SiC, the N_C is more stable than the N_{Si}. The N_C introduced shallow donor level during ion implantation and its high concentration could pave way for a desirable high conductivity device application. Nitrogen has also be reported to form clusters or complexes with nitrides such as vacancies or antisite, therefore having lower energy. In addition, defect-complex

may also introduced deep level in the band gap of 4*H*-SiC which acts as a recombination centre. Recent report on characterisation and formation of NV centre in 3 polytypes (3*C*, 4*H* and 6*H*) of SiC by Csore *et al.* [19] reveals that for 3*C*-SiC, the energy of the acceptor level of NV defect is E_V+1.5 eV and with an excited state resonance close to the conduction band minimum (CBM). In addition, various reports suggest that the 4*H*-SiC with the largest band gap compared to the 3*C* and 6*H* is the optimal host for NV centre quantum bits (qubit) application [20, 21]. Except for the NV centre (N_CV_{Si}) in 3*C*-SiC and 4*H*-SiC detailed information about the structural, electronic and thermal properties of N_CV_C, $N_{Si}V_C$, $N_{Si}V_{Si}$, B_CV_C, B_CV_{Si}, $B_{Si}V_C$ and $B_{Si}V_{Si}$ are lacking and needed to be studied, hence the motivation for this study.

Using a hybrid density functional, we show that the N_CV_C, N_CV_{Si}, $N_{Si}V_{Si}$, B_CV_C, $B_{Si}V_C$ and $B_{Si}V_{Si}$ are stable vacancy-complexes with binding energies within the range of 0.10 to 3.50 eV for N related vacancy-complexes, and 0.10 to 2.74 eV for B related vacancy-complexes. The $N_{Si}V_{Si}$ and $B_{Si}V_{Si}$ have higher formation energies with low binding energies. The defects investigated were assessed further on the basis of their charge states and thermodynamic transition energy levels. We have shown that both the B and N related complexes exhibit charge states controlled metastability behaviour.

2. Computational details

A density function theory modelling of the structural electronic and charge state thermodynamic electrical levels of N and B related vacancy-complexes in 4*H*-SiC was

performed using the Vienna *ab-initio* Simulation Package (VASP) [22, 23]. In order to separate the core electrons from the chemically active valence electron, the projector-augmented wave (PAW) method [22, 24] was used. The $2s^2$, $2p^1$ for the B, $2s^2$, $2p^2$ for the C, $2s^2$, $2p^3$ for the N and $3s^2$, $3p^2$ electrons for the Si, were included in our calculations as valence electrons. All calculations were performed using the HSE06 [25] hybrid functional with generalized gradient approximation (GGA) functional of Perdew, Burke and Ernzerhof (PBE) [26]. Based on the HSE06 approach, the local DFT exchange potential was mixed with the non-local exact exchange potential. This is basically governed by adjustable parameter which is an integral component of the HSE06. For all calculations, a 25% of the non-local exact exchange potential was used, as it reproduced a band gap 3.23 eV which is consistent with other reported theoretical results [20, 27] and close to the experimental band gap of 3.26 eV [28]. In addition, the HSE has been used to accurately predict several wide and narrow band gap semiconductor materials [29, 30]. The $4H$-SiC has a hexagonal cubic structure with the space group $P_{6_}3mc$ for its unit cell. For defect modelling, it is required to optimised the unit cell. The optimised lattice constants and band gaps for the $4H$-SiC unit cell were obtained using a Monkhorst-Pack [31] grid of $8 \times 8 \times 8$. A kinetic energy cutoff of 400 eV was used for the expansion of one-electron Kohn-Sham wave functions on the plane-wave basis. Furthermore, the $4H$-SiC unit cell was relaxed until the minimum total energy difference was less than 10^{-5} eV. Equilibrium configuration of the atomic structure was allowed to relax freely until the Hellmann-Feynman forces acting on each atom was less than 0.01 eV/Å.

To explore the defect properties, a supercell containing 96 atoms (for which 48 atoms are Si and the remaining atoms are C) which was obtained by repeating the structure of the perfect 4H-SiC unit cell was used. The 96 atoms supercell was adopted after convergence test which was carried out in order to reduced the effect of defect-defect interactions shown that it is sufficient to model defect properties. For example, the formation energies of the neutral charge state of V_C were calculated for the 72, 96, 144, 288 and 576 atoms supercells with energies of 5.25, 5.00, 5.29, 5.63 and 5.84 eV, respectively. For the V_{Si}, the formation energy of the neutral charge state for the 72, 96, 144, 288 and 576 atoms supercells are 7.36, 7.23, 7.37, 7.35 and 7.56 eV, respectively. The 96 atoms supercell was relaxed with a plane wave energy cut-off of 400 eV and a $2 \times 2 \times 2$ Monkhorst-Pack [31] k-point grid was used to sample the Brillouin zone. All atoms in the supercell were fully relaxed with convergence criteria of a minimum total energy difference less than 10^{-5} eV and the force on each ion less than 0.01 eV/Å. In the case of the V_{Si} related defect-complexes, the error of neglecting spin polarization is known from the work of Zywietz *et al* [32]. Reports based on the V_{Si} have shown that this defect has a ground state with total spin $\frac{3}{2}$ [33, 34, 35]. In this report, spin polarisation was included in all calculations involving V_{Si} related vacancy-complexes to account for its spin dependency. According to Boltzmann distribution, a defect free energy (G^F) is related to the defect concentration (D_{conc}) as

$$D_{conc} = N_0 \exp(-G^F/k_B T), \tag{1}$$

where N_0 is the number of possible defects sites per bulk quanta that a defect can

occur, K_B (eV/K) is the Boltzmann constant and T is temperature in Kelvin. The defect free energy G^F for crystalline solid under moderate temperature and pressure is approximated to the formation energy (E^F) of a defect i.e $G^F \approx E^F$. In a compound semiconductor (4*H*-SiC), the equilibrium defects concentration depends on the chemical environment such as Si and C chemical potentials, μ_{Si} and μ_C, respectively. The μ_{Si} and μ_C may vary within a given bounds in order to prevent undesired formation of more stable phases other than SiC. The difference between the energies of a Si-C (μ_{SiC}^{bulk}) pair and the sum of a C and a Si atom in their standard states, μ_C^{bulk} and μ_{Si}^{bulk}, respectively is the enthalpy or heat of formation (H^F) given as:

$$H^F = \mu_C^{bulk} + \mu_{Si}^{bulk} - \mu_{SiC}^{bulk}. \tag{2}$$

From the above, the chemical potential are then written as

$$\mu_C = \mu_C^{bulk} - \frac{1}{2}H^F - \frac{1}{2}\triangle\mu, \tag{3}$$

$$\mu_{Si} = \mu_{Si}^{bulk} - \frac{1}{2}H^F + \frac{1}{2}\triangle\mu, \tag{4}$$

where the $\triangle\mu$ is $-H^F$, 0 and H^F for C-rich, stoichiometric and Si-rich material, respectively. While the chemical potentials of Si and C, that is the μ_{Si}^{bulk} and μ_C^{bulk} were respectively calculated using the bulk silicon and diamond (as the small difference in the energy of diamond and graphite introduced less significant error) structure respectively, the μ_{SiC}^{bulk} was calculated using the hexagonal cubic structure. For us to set the upper bound on the N chemical potential (μ_N) the hexagonal β-Si_3N_4 (since it serves as the solubility−limiting phase in SiC) was used as its chemical potential reference. The

μ_N was calculated and obtained to be -12.22 eV, this is in accordance to the result of ref. [19]. The μ_B was obtained as the total energy per B atom (i.e $\frac{E^{total}}{N}$; where E^{total} is the total energy and N is the number of B atoms) from the α-rhombohedral boron structure. By using μ_{SiC}^{bulk}=-17.47, μ_{Si}^{bulk}=-6.30 eV and μ_{C}^{bulk}=-10.55 eV, we obtained the H^F= 0.62 eV. This is in good agreement with earlier reported theoretical results [32, 36, 37]. Reports have shown that for the $\mathrm{V_C}$ and $\mathrm{V_{Si}}$, the most energetically favourable conditions with respect to formation energy occurs under Si-rich and C-rich conditions, respectively [38, 39, 40]. In our calculations, the formation energies of the defect-complexes formed with $\mathrm{V_C}$ and $\mathrm{V_{Si}}$ were obtained under Si-rich and C-rich conditions, respectively, which are in agreement with literature [41, 42].

Under equilibrium conditions, the defect formation and thermodynamic charge state transition energy level ($\epsilon(q/q')$) are calculated from the total energy (E(D,q)) for a supercell containing the optimized defect D in its charge state q. The defect formation energy E^F as a function of electron Fermi energy (ε_F) is given as [6]

$$E^F(D,q) = E(D,q) - E(4H - SiC) + \sum_i (\triangle n)_i \mu_i + q\mu_e + E^q_{cor}, \qquad (5)$$

where $E(4H\text{-}SiC)$ is the total energy of the non-defect 96 atoms supercell of $4H$-SiC and the $(\triangle n)_i$ is the difference in the number of constituent atoms of type i between the 96 atoms supercell of $4H$-SiC and the supercell containing the vacancy-complexes. While the chemical potential of different constituent atoms is represented as μ_i, the electron chemical potential μ_e is defined as

$$\mu_e = E_V + \varepsilon_F, \qquad (6)$$

where E_V is used to align the bulk VBM to that of the defect supercell and ε_F is the Fermi energy, which is varied from the valence band edge to the conduction band minimum (CBM). We have included the correction term E^q_{cor} to Eq. 5 according to the Freysoldt *et al* [43, 44] method. The E^q_{cor} accounts for the deficiency surrounding the calculation of defect energy of formation due to errors from the finite-size effects within the supercell and electrostatic potential. A defect charge states thermodynamic transition energy level $\epsilon(q/q')$ is the Fermi energy for which the formation energies of two charge states say q and q' are equal. The $\epsilon(q/q')$ is given as [7, 43, 44]

$$\epsilon(q/q') = \frac{E^F(D, q;\ \varepsilon_F = 0) - E^F(D, q';\ \varepsilon_F = 0)}{q' - q}. \tag{7}$$

In this report, we focus on two different defect-complexes by replacing either one Si or C atom with one impurity atom and simultaneously removing either a Si or a C atom to form vacancy-complexes. For a defect-complex, it is important to check if the parent complex will dissociate into well non-interacting defects. This is ascertained by calculating the binding energy. For a defect-complex (XY) with an energy of formation E^F_{XY}, the binding energy E_B is given as

$$E_B = \sum_{i=1}^{n} E^F_{X_i} - E^F_{XY}, \tag{8}$$

where $E^F_{X_i}$ is the formation energy of the *ith* non-interacting defect. According to Eq. 8, if $E_B > 0$ then the formation of XY defect-complex is favourable. Otherwise dissociation is imminent with a lower energy than the energy of formation.

3. Results and Discussion

Fig. 1 displays the model of a 4*H*-SiC unit cell, possible configurations of defect-complex in 4*H*-SiC, boron substitution at Si site and boron vacancy-complex ($B_{Si}V_C$). The calculated Si-C bond distance for the pristine 4*H*-SiC is 1.89 Å (see Fig. 1a) which is in agreement with experimental result [45]. The calculated lattice constant 3.07 and 10.05 Å for a and c, respectively. These are in agreement with previous results reported [28, 46]. In this report, defects present in B-implanted or N-implanted in a 4*H*-SiC device are of interest. The initial calculations focused on defects containing N or B at a substitutional site with either a C or Si vacancy: forming a vacancy-complex (N_CV_C, N_CV_{Si}, $N_{Si}V_C$, $N_{Si}V_{Si}$, B_CV_C, B_CV_{Si}, $B_{Si}V_C$ and $B_{Si}V_{Si}$). Table 1 displays the relaxed bond distance of impurity and host atom in Å. The bond lengths were calculated with respect to impurities nearest neighbour Si or C atom as displayed by Fig. 1c and 1d . The calculated relaxed bond distance of B-C for $B_{Si}V_C$ ($B_{Si}V_{Si}$), N-C for $N_{Si}V_C$ ($N_{Si}V_{Si}$), B-Si for B_CV_C (B_CV_{Si}) and N-Si for N_CV_C ($N_{Si}V_{Si}$) are respectively, 1.63 (1.80), 1.60 (1.69), 1.91 (1.97) and 1.80 (1.78). These bond lengths are 13.70 (4.70)%, 16.00 (11.00)%, 1.00 (4.50)% and 4.20 (5.6)%, respectively different from that of the bond length of Si-C. The difference in bond length can be attributed to the different sizes of the impurity atom that was introduced and host atoms that were removed from the pristine 4*H*-SiC. Due to the small atomic size of the N atom relative to the B, C and Si, we expected the systems with N related impurity to experienced more induced strains than the others. This could account for the possible higher energy of formation

observed for the N related vacancy-complexes than the B vacancy-complexes.

For us to pay proper attention and present a scientific insight into the formation energy of the defect-complexes, we have calculated the formation energy of the neutral charge state of V_C and V_{Si} to be 5.00 and 7.23 eV which are in good agreement with earlier reported results [27, 33, 47].

3.1. N vacancy-complexes in 4H-SiC

In this section, we have investigated four different vacancy-complexes formed by N and V_{Si} or V_C: (N_CV_C, N_CV_{Si}, $N_{Si}V_C$ and $N_{Si}V_{Si}$). Table 2 (calculated under defect rich conditions) lists the formation energy and binding energy at $\varepsilon_F = 0$ of the vacancy-complexes formed by N and B in 4*H*-SiC.

The so called NV centre (N_CV_{Si}) in 4*H*-SiC is a well known defect, which has been extensively studied [2, 19, 20]. In this article, we have reported a few findings about the NV centre in 4*H*-SiC which are in agreement with earlier reports. For example, the calculated 6.81 and 3.81 eV corresponding to the formation and binding energies of the NV centre in 4*H*-SiC are in agreement with previous theoretical results [19]. The thermodynamic charge state transition levels observed for the NV centre are $(0/-)$ and $(-/--)$ with energies of E_V+1.45 and E_V+2.66 eV, respectively. The deep double acceptor levels $(0/-)$ and $(-/--)$ of the NV centre have been theoretically predicted [2, 19, 20]. While according to Csore *et al.* [19], the $(0/-)$ and $(-/--)$ has an energy level within 1.46-1.55 and 2.42-2.65 eV, respectively above the VBM, Weber

et al. [20] reported the energy levels of the (0/−) and (−/−−) transition states to be 1.2 and 0.7 eV below the CBM.

To further explore other vacancy-complexes, we investigated the $N_C V_C$ vacancy-complex. The $N_C V_C$ under equilibrium conditions for the neutral charge state has a formation energy of 6.45 eV. This value is 0.36 eV slightly lower than that of the NV centre. The binding energy of the $N_C V_C$ is 0.85 eV whereas for the NV centre, it is 3.81 eV. This suggests that the energy required to split the vacancy-complex would be lower for the $N_C V_C$ than the NV centre. The $N_C V_C$ induced energy levels in the band gap of 4*H*-SiC. The first noticeable energy level close to the VBM is the (++/+) with a deep energy of E_V+1.11 eV. As the Fermi energy is varied, the (+/0) deep donor transition state with energy of E_V+2.15 eV is observed. Further varying the Fermi energy close to the band edge, the (0/−) shallow acceptor level close to the CBM with energy of E_C−0.13 eV is observed.

The $N_{Si} V_C$ is another vacancy-complex which its defect activities were explored. The $N_{Si} V_C$ under equilibrium conditions, has a formation energy of 10.89 eV and a binding energy of 3.50 eV for the neutral charge state (see Table 2). The $N_{Si} V_{SC}$ introduced two defect levels in the band gap of 4*H*-SiC that are deep for the (++/+) and (+/0), and shallow for the (0/−) transition states. While the (++/+) and (+/0) donor levels have energy levels of E_V+1.45 eV and E_V+2.08 eV respectively, the (0/−) an acceptor level has an energy level of E_C−0.22 eV.

The $N_{Si} V_{Si}$ is a unique kind of defect: where silicon is substituted by N and a silicon

atom is removed to form a vacancy. This defect has a high formation energy (17.59 eV) relative to the N_CV_C, N_CV_{Si} and $N_{Si}V_C$, and with a low binding energy of 0.10 eV. The implication of the high formation energy is that under equilibrium conditions, the concentration of the defect which is proportional to the $\exp(\frac{-G^F}{K_BT})$ is expected to be extremely low compared to others. Considering the fact that the N_C and V_C are more energetically favourable than the N_{Si} and V_{Si} under their chemical rich conditions. We expected the $N_{Si}V_{Si}$ to have a higher formation energy than the other N related vacancy-complexes reported. Whereas the (+/0) donor level of the $N_{Si}V_{Si}$ is more stable close to the VBM with a shallow energy of E_V+0.50 eV, the double acceptor level (0/−) and (−/−−) are located deep within the band gap with energies E_V+1.50 and E_C−0.72 eV, respectively.

More insight into the N related vacancy-complexes reveal that for all charge states, the $N_{Si}V_{Si}$ has the highest formation energy. This suggests that its concentration for all charge states is relatively lower than the other N-related defect complexes. The order of sequence of formation energy under equilibrium conditions for the neutral charge state of N-related vacancy-complexes is N_CV_C $<N_CV_{Si}<N_{Si}V_C<$ $N_{Si}V_{Si}$. This suggests the possible reason why the N_C during ion implantation is preferable than the N_{Si}. The N_CV_C and N_CV_{Si} with higher concentrations than the $N_{Si}V_C$ and $N_{Si}V_{Si}$ may be desirable in devices region where high conductivity is required. As displayed by Fig. 3a, close to the VBM the double positive charge state of the N_CV_C is the most stable. As the Fermi energy is varied deep in the band gap from the VBM, at energy level of 1.11 eV, the

single negative charge state of the N_CV_{Si} becomes more stable. Furthermore, varying the Fermi energy close to the CBM, the double negative charge state of the N_CV_{Si} becomes more stable.

3.2. B vacancy-complexes 4H-SiC

In this part of the paper, we present results of four different vacancy-complexes formed by B and V_{Si} or V_C in 4*H*-SiC: B_CV_C, B_CV_{Si}, $B_{Si}V_C$ and $B_{Si}V_{Si}$.

As listed in Table 2, for the neutral charge state, the most stable vacancy-complex is the B_CV_C with binding energy of 2.59 eV and a formation energy which is 0.22 eV lower than that of the $B_{Si}V_C$. The $B_{Si}V_{Si}$ with binding energy of 0.10 eV has the highest formation energy of 11.52 eV compared to other B related vacancy-complexes. The positive binding energies of the B related vacancy-complexes suggest that these defects are stable and hence dissociating into well non-interacting defects will occur at the expense of a higher energy. The deep levels induced by the B_CV_C are 1.62 and 2.72 eV above the VBM for the (+/0) and (0/−), respectively. The B_CV_{Si} is a shallow donor (+/0) level with an energy 0.19 eV above the VBM. There is no evidence of double donor level induced in all B related complexes. However, the B_CV_{Si} exhibited a double acceptor level. The B_CV_{Si} double acceptor levels of (0/−) and (−/−−) where deep lying inside the band gap with energy of E_V+1.24 and E_V+2.28, respectively. For the $B_{Si}V_C$, Deak *et al.* reported the $B_{Si}V_C$ to induced (0/−) level with 2.1 eV above the VBM [48]. The idea here is to extend the work of Deak by using the more accurate HSE hybrid

functional to predict the energy levels of the $B_{Si}V_C$. In this report, the vacancy-complex $B_{Si}V_C$ induced two deep defect levels, the (+/0) and (0/−) lying in the band gap with 1.83 and 2.80 eV above the VBM, respectively. The different energy levels observed in our report and that of Ref [48] could be attributed to the DFT problem with LDA, as DFT with LDA inaccurately predicts the band gap of materials. Consequently, one should expect DFT with LDA to wrongly predict the electrical induced defect levels in the band gap of materials. For the $B_{Si}V_{Si}$, double acceptor levels with energies of E_V+0.94 and E_V+2.00 eV, respectively for the (0/−) and (−/−−) were observed. As shown by Fig 3b, the single positive charge state of the B_CV_C and $B_{Si}V_C$ are more stable from the valence band maximum. However, as the Fermi energy is varied the neutral charge state of the $B_{Si}V_C$ becomes more energetically stable up to energy of 2.28 eV above the VBM. Furthermore, as the Fermi energy is varied close to the conduction band minimum, the single negative charge state of the $B_{Si}V_C$ becomes energetically more stable.

3.3. Metastability of B and N vacancy-complexes in 4H-SiC

Metastability of charge states in a point defect (vacancy, interstitials, interstitial-complex, vacancy-complexes) has been reported for Si [49, 50], Ge [8, 6, 51] and SiC [52, 53, 54, 55]. A defect with metastable properties can exist in more than a configuration with different charge states [51]. A defect may be stable with the lowest formation energy in a particular charge state, but when the charge state is change,

the defect becomes unstable in that configuration. For boron-vacancy complex in Si, two distinct metastable configurations have been observed in two different atomic defect charge states. These two different configurations have lowest energies in two different distinct charge states. This is achievable by annealing with or without bias in a deep-level transient spectroscopy (DLTS) measurement. Many reports on charge state controlled metastable defects in SiC have been documented [52, 53, 54, 55]. Since we have shown that the N_CV_{Si}, N_CV_C, $B_{Si}V_C$ and B_CV_C are stable with positive binding energies, hence: the lowest energy configuration needs to be examined. Table 4 displays the calculated formation energies of the B and N vacancy-complexes for different configurations in charge state −1, 0 and +1. While experimental observation has shown that B vacancy-complex have two metastable configurations in Si, in this report, we show that $B_{Si}V_C$ and B_CV_C are metastable defects. As displayed in Fig. 3a, we observed that as $\varepsilon_F \Rightarrow E_V$, the +2 and +1 charge states of the N_CV_C are the minimum energies at distinct Fermi energy. On the other hand, the −1 and −2 charge states of the N_CV_{Si} are the lowest energies configuration at a distinct Fermi energy as the $\varepsilon_F \Rightarrow E_C$. In a typical DLTS spectrum measurements, the deep levels of the metastable configurations of N related defect complex in 4*H*-SiC give rise to high temperature peaks (low emission rate peaks in isothermal Laplace DLTS measurement). According to Fig. 3b, as the ε_F approaches the E_V, the +1 charge state of the B_CV_C is the minimum energy configuration whereas as the the ε_F approaches the E_C the neutral and −1 charge states of the $B_{Si}V_C$ are the least formation energies configuration at

different Fermi energies. In DLTS experimental measurements, ε_F approaches E_C and ε_F approaches E_V are analogue to reverse and forward bias, respectively. A reverse bias applied to a Schottky diode increases the band bending by shifting the conduction band below the Fermi level. The result is the depletion width with defect levels in the band gap emitting holes (capturing electrons). The difference between the formation energy of the +1, 0 and −1 charge states of the $B_{Si}V_C$ and B_CV_C are within the order of $3k_BT$ or less. This suggests that both configurations can be observed experimentally.

4. Summary

We have used HSE06 hybrid density functional from first principle approach to study the properties of various N and B related vacancy-complexes in 4*H*-SiC. The formation energies and charge state thermodynamic transition levels induced in the band gap were reported. The B related vacancy-complexes formed with V_C are more energetically favourable in all charge states than those vacancy-complexes formed with V_{Si}. While the N_CV_C is the most energetically stable N related vacancy-complex for the neutral charge state, the $B_{Si}V_C$ on the other hand is energetically the most favourable B related vacancy-complex in its neutral charge state. All B and N vacancy-complexes in this report are stable with respect to their binding energies. Except for the N_CV_C and B_CV_{Si} which induced shallow levels close to the CBM and VBM respectively, other B and N related vacancy-complexes exhibited deep centre behaviour in the band gap of 4*H*-SiC. The B and N related vacancy-complexes exhibited charge state controlled

metastability behaviours

5. Acknowledgement

This work is based on the research supported partly by National Research foundation (NRF) of South Africa (Grant specific unique reference number (UID) 98961). The opinions, findings and conclusion expressed are those of the authors and NRF accepts no liability whatsoever in this regard.

[1] E. Omotoso, W.E. Meyer, P.J. Janse van Rensburg, E. Igumbor, S.M. Tunhuma, P.N.M. Ngoepe, H.T. Danga, and F.D. Auret. *Nuclear Instruments and Methods in Physics Research Section B: Beam Interactions with Materials and Atoms*, 409:241 – 245, 2017.

[2] J Cottom, G Gruber, P Hadley, M Koch, G Pobegen, T Aichinger, and A Shluger. *Journal of Applied Physics*, 119(18):181507, 2016.

[3] HT Danga, FD Auret, SM Tunhuma, E Omotoso, E Igumbor, and WE Meyer. Thermal stability of defects introduced by electron beam deposition in p-type silicon. *Nuclear Instruments and Methods in Physics Research Section B: Beam Interactions with Materials and Atoms*, 409:46–49, 2017.

[4] H.T. Danga, F.D. Auret, S.M. Tunhuma, E. Omotoso, E. Igumbor, and W.E. Meyer. *Nuclear Instruments and Methods in Physics Research Section B: Beam Interactions with Materials and Atoms*, 409:46 – 49, 2017.

[5] Zhimin Li, Wancheng Zhou, Xiaolei Su, Fa Luo, Yunxia Huang, and Cheng Wang. *Journal of Alloys and Compounds*, 509(3):973–976, 2011.

[6] Emmanuel Igumbor, Refilwe Edwin Mapasha, Richard Andrew, and Walter Ernst Meyer. *Computational Condensed Matter*, 8:31–35, 2016.

[7] E Igumbor and WE Meyer. *Materials Science in Semiconductor Processing*, 43:129–133, 2016.

[8] Emmanuel Igumbor, Refilwe Edwin Mapasha, and Walter Ernst Meyer. *Journal of Electronic Materials*, 46(7):3880–3887, 2017.

[9] Zhimin Li, Wancheng Zhou, Xiaolei Su, Fa Luo, Dongmei Zhu, and Pengle Liu. *Journal of the American Ceramic Society*, 91(8):2607–2610, 2008.

[10] Simeon Agathopoulos. *Ceramics International*, 38(4):3309 – 3315, 2012.

[11] Riccardo Rurali, Philippe Godignon, J Rebollo, P Ordejón, and E Hernández. *Applied physics letters*, 81(16):2989–2991, 2002.

[12] B Aradi, Adam Gali, P Deák, NT Son, and Erik Janzén. *Physica B: Condensed Matter*, 308:722–725, 2001.

[13] DJ Larkin. *physica status solidi (b)*, 202(1):305–320, 1997.

[14] A Gali, P Deák, RP Devaty, and WJ Choyke. *Physical Review B*, 60(15):10620, 1999.

[15] H Tahini, A Chroneos, RW Grimes, U Schwingenschlögl, and H Bracht. *Applied Physics Letters*, 99(7):072112, 2011.

[16] A Chroneos. *Journal of applied physics*, 105:056101, 2009.

[17] José Coutinho, Vitor JB Torres, Sven Öberg, Alexandra Carvalho, Colin Janke, Robert Jones, and Patrick R Briddon. *Journal of Materials Science: Materials in Electronics*, 18(7):769–773, 2007.

[18] A Gali, T Hornos, P Deák, NT Son, Erik Janzén, and WJ Choyke. *Applied Physics Letters*, 86(10):102108, 2005.

[19] A Csóré, HJ Von Bardeleben, JL Cantin, and A Gali. *arXiv preprint arXiv:1705.06229*, 2017.

[20] JR Weber, WF Koehl, JB Varley, A Janotti, BB Buckley, CG Van de Walle, and DD Awschalom. *Journal of Applied Physics*, 109(10):102417, 2011.

[21] Xiaopeng Wang, Mingwen Zhao, Hongxia Bu, Hongyu Zhang, Xiujie He, and Aizhu Wang. *Journal of Applied Physics*, 114(19):194305, 2013.

[22] Georg Kresse and Jürgen Furthmüller. *Physical Review B*, 54(16):11169, 1996.

[23] Georg Kresse and D Joubert. *Physical Review B*, 59(3):1758, 1999.

[24] Peter E Blöchl. Projector augmented-wave method. *Physical Review B*, 50(24):17953, 1994.

[25] Jochen Heyd, Gustavo E. Scuseria, and Matthias Ernzerhof. *The Journal of Chemical Physics*, 118(18):8207–8215, 2003.

[26] John P. Perdew, Kieron Burke, and Matthias Ernzerhof. *Phys. Rev. Lett.*, 77:3865–3868, 1996.

[27] L Gordon, Anderson Janotti, and Chris G Van de Walle. *Physical Review B*, 92(4):045208, 2015.

[28] Michael E Levinshtein, Sergey L Rumyantsev, and Michael S Shur. John Wiley & Sons, 2001.

[29] Peter Deák, Bálint Aradi, Thomas Frauenheim, Erik Janzén, and Adam Gali. *Phys. Rev. B*, 81:153203, 2010.

[30] E Igumbor, CNM Ouma, G Webb, and WE Meyer. *Physica B: Condensed Matter*, 480:191–195, 2016.

[31] Hendrik J. Monkhorst and James D. Pack. *Phys. Rev. B*, 13(12):5188–5192, 1976.

[32] A Zywietz, J Furthmüller, and F Bechstedt. *Physical Review B*, 59(23):15166, 1999.

[33] ÖO Soykal, Pratibha Dev, and Sophia E Economou. *Physical Review B*, 93(8):081207, 2016.

[34] Pavel G. Baranov, Anna P. Bundakova, Alexandra A. Soltamova, Sergei B. Orlinskii, Igor V. Borovykh, Rob Zondervan, Rogier Verberk, and Jan Schmidt. 83(12):125203, 2011.

[35] N Mizuochi, S Yamasaki, H Takizawa, N Morishita, T Ohshima, H Itoh, and J Isoya. *Physical Review B*, 66(23):235202, 2002.

[36] Michel Bockstedte, Alexander Mattausch, and Oleg Pankratov. *Physical Review B*, 68(20):205201, 2003.

[37] TT Petrenko and TL Petrenko. *Physical Review B*, 93(16):165203, 2016.

[38] Jun-Ichi Iwata, Chikara Shinei, and Atsushi Oshiyama. *Physical Review B*, 93(12):125202, 2016.

[39] David Shrader, Sarah M Khalil, Tyler Gerczak, Todd R Allen, Andrew J Heim, Izabela Szlufarska, and Dane Morgan. *Journal of Nuclear Materials*, 408(3):257–271, 2011.

[40] L Torpo, M Marlo, TEM Staab, and RM Nieminen. *Journal of Physics: Condensed Matter*, 13(28):6203, 2001.

[41] B Aradi, A Gali, P Deák, JE Lowther, NT Son, Erik Janzén, and WJ Choyke. *Physical Review*

B, 63(24):245202, 2001.

[42] Masanori Miyata and Yoshinori Hayafuji. *Applied physics express*, 1(11):111401, 2008.

[43] Christoph Freysoldt, Jrg Neugebauer, and Chris G. Van de Walle. *physica status solidi (b)*, 248(5):1067–1076, 2011.

[44] Yu Kumagai and Fumiyasu Oba. *Phys. Rev. B*, 89:195205, 2014.

[45] Ming Yu, CS Jayanthi, and SY Wu. *arXiv preprint arXiv:0901.3567*, 2009.

[46] Jakub Sotys, Jacek Piechota, Pawe Strak, and Stanisaw Krukowski. *Applied Surface Science*, 393:168 – 179, 2017.

[47] JR Weber, WF Koehl, JB Varley, A Janotti, BB Buckley, CG Van de Walle, and David D Awschalom. *Proceedings of the National Academy of Sciences*, 107(19):8513–8518, 2010.

[48] Peter Deák, Bálint Aradi, and Adam Gali. *Journal of Physics: Condensed Matter*, 13(40):9019, 2001.

[49] J Adey, R Jones, DW Palmer, PR Briddon, and S Öberg. *Physical Review B*, 71(16):165211, 2005.

[50] Peter Deák, Adam Gali, András Sólyom, Adam Buruzs, and Thomas Frauenheim. *Journal of Physics: Condensed Matter*, 17(22):S2141, 2005.

[51] Emmanuel Igumbor, Richard Charles Andrew, and Walter Ernst Meyer. *Journal of Electronic Materials*, 46(2):1022–1029, 2017.

[52] R Devanathan, WJ Weber, and F Gao. *Journal of Applied Physics*, 90(5):2303–2309, 2001.

[53] E Rauls, Th Lingner, Z Hajnal, S Greulich-Weber, Th Frauenheim, and J-M Spaeth. *physica status solidi (b)*, 217(2), 2000.

[54] A Gali, NT Son, and Erik Janzén. *Physical Review B*, 73(3):033204, 2006.

[55] CG Hemmingsson, NT Son, Olle Kordina, and Erik Janzén. *Journal of applied physics*, 91(3):1324–1330, 2002.

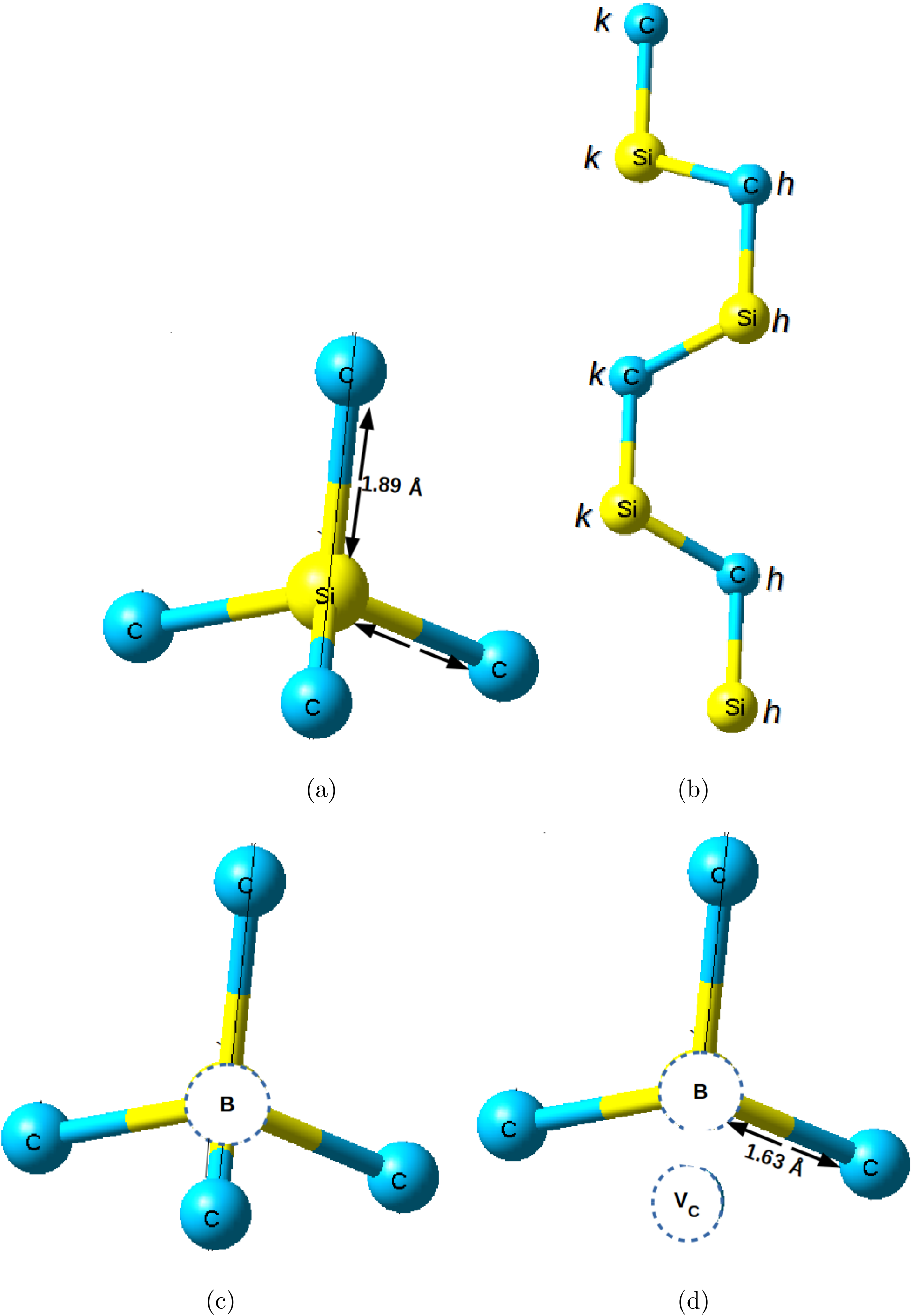

Figure 1. Model of (a) unit cell 4*H*-SiC (b) possible configurations of defect-defect complex in 4*H*-SiC (c) boron substitution in 4*H*-SiC and (d) boron vacancy-complex in 4*H*-SiC.

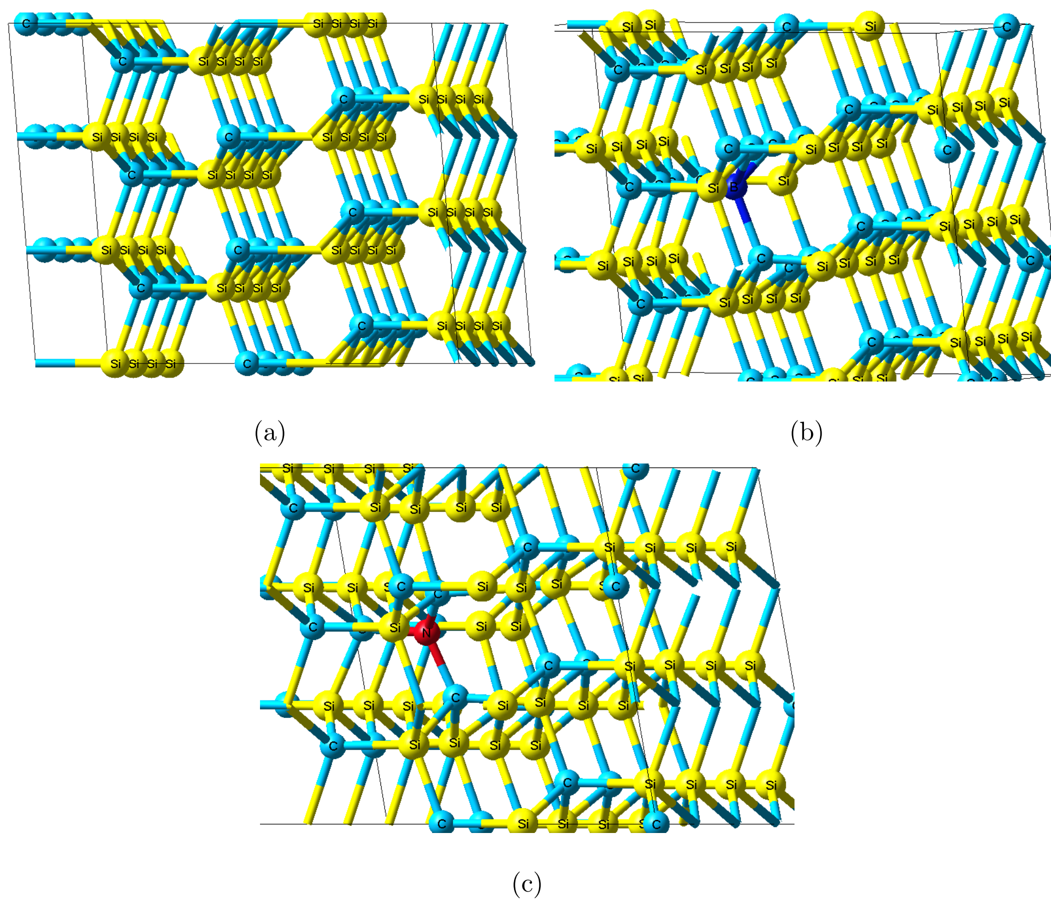

Figure 2. Fully relaxed geometric structure of (a) pristine 96 atoms supercell 4*H*-SiC; (b) 4*H*-SiC supercell with a boron substitutional defect at the Si atom site and a Si vacancy (c) 4*H*-SiC supercell containing N substitutional defect at the Si atom site and a C vacancy.

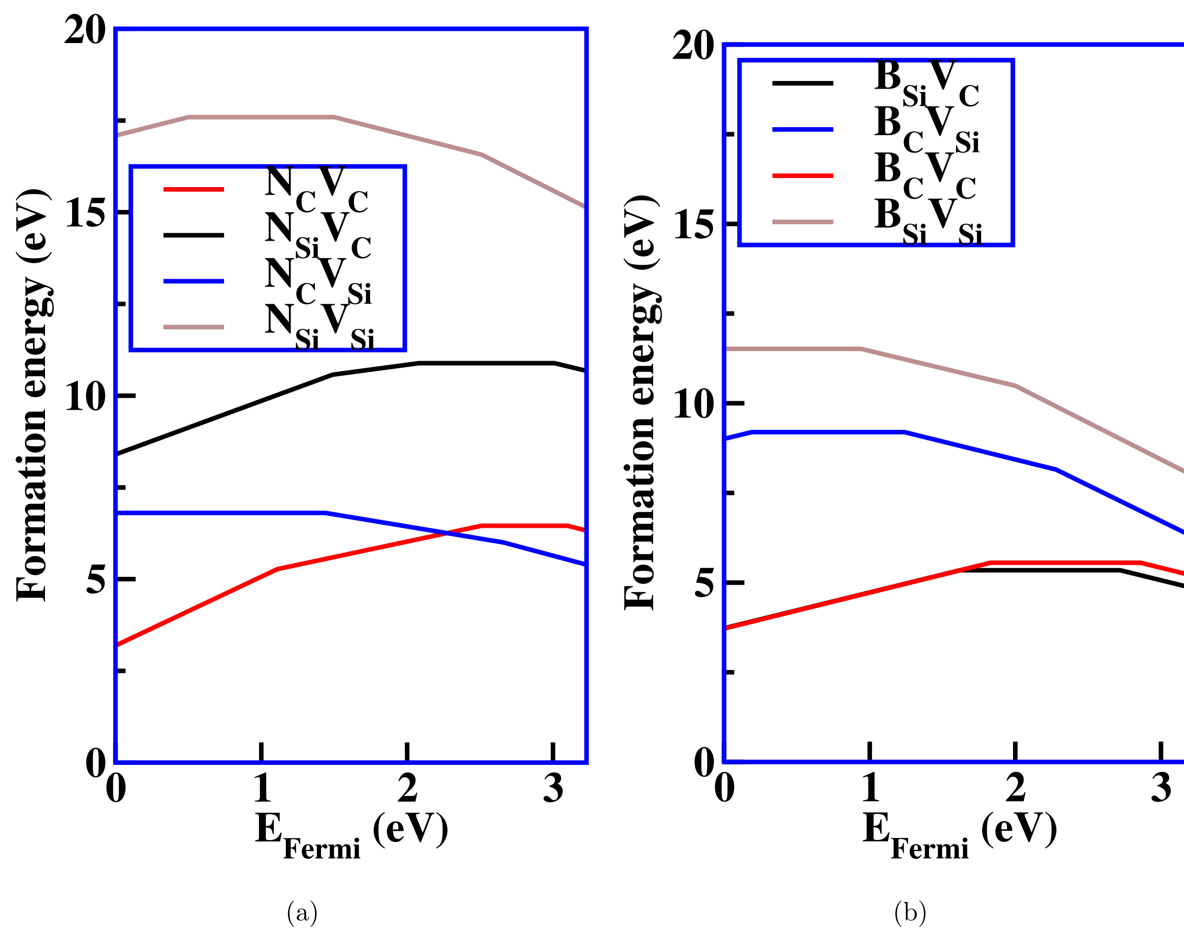

Figure 3. Plots of formation energy as a function of the Fermi energy for vacancy-complexes in 4*H*-SiC. The slope of each graph corresponds to the charge state as defined in Eq. 5. The defect levels of vacancy-complexes formed with V_{Si} were obtained under C-rich conditions, whereas the defect levels of vacancy-complexes formed by V_C were calculated under Si-rich conditions.

Table 1. The relaxed bond distance of impurity and host atom in Å. The bond lengths were calculated with respect to impurities nearest neighbour Si (in bold) or C atom.

N_CV_{Si}	$N_{Si}V_{Si}$	N_CV_C	$N_{Si}V_C$
1.78	1.69	1.80	**160**
B_CV_{Si}	$B_{Si}V_{Si}$	B_CV_C	$B_{Si}V_C$
1.97	1.80	**1.91**	1.63

Table 2. The formation energy (E^F) and binding energy (E_B) in eV at $\varepsilon_F = 0$ of vacancy-complexes formed by N and B in $4H$-SiC. The E^F and E_B energies were calculated under chemical potential, i.e the vacancy-complexes formed with V_{Si} were calculated under C-rich conditions and those formed with V_C were calculated under Si-rich conditions.

	N_CV_{Si}	N_CV_C	$N_{Si}V_C$	$N_{Si}V_{Si}$
E^F	6.81	6.45	10.89	17.59
E_B	3.81	0.85	3.50	0.10
	B_CV_{Si}	B_CV_C	$B_{Si}V_C$	$B_{Si}V_{Si}$
E^F	9.20	5.34	5.56	11.52
E_B	1.95	2.59	2.74	0.10

Table 3. Table showing the charge state transition ($\varepsilon(q/q')$) levels above the VBM in eV induced by B and N vacancy-complexes in $4H$-SiC.

$\varepsilon(q/q')$	N_CV_{Si}	N_CV_C	$N_{Si}V_C$	$N_{Si}V_{Si}$	B_CV_C	B_CV_{Si}	$B_{Si}V_C$	$B_{Si}V_{Si}$
$(++/+)$	–	1.11	1.45	–	–	–	–	–
$(+/0)$	–	2.15	2.08	0.50	1.62	0.19	1.83	–
$(0/-)$	1.45	3.10	3.01	1.50	2.72	1.24	2.86	0.94
$(-/--)$	2.66	–	–	2.51	–	2.28	–	2.00

Table 4. Calculated formation energies in eV of the B and N vacancy-complexes in 4*H*-SiC for different configurations. The charge state with the lowest energy for each configuration is shown in bold.

Configuration	−1	0	+1
$N_C V_{Si}$	**8.19**	6.81	6.68
$N_C V_C$	9.55	**6.45**	**4.30**
$B_{Si} V_C$	8.10	5.56	**3.72**
$B_C V_C$	**8.06**	**5.34**	3.73